J Korean Med Sci 2000; 15: 494-500
ISSN 1011-8934

Cellular Electrophysiology of Fast Pathway Ablation of Rabbit Atrioventricular Node

Discrete radiofrequency lesion at the atrial insertion site of the tendon of Todaro in the perfused rabbit preparation lengthens A-H interval, mimicking fast pathway input ablation. This study attempts to define the cellular electrophysiology of the ablation region prior to and after the elimination of fast AV node conduction. In six superfused rabbit AV node preparations, the cellular electrophysiology around the region of the atrial insertion to the tendon of Todaro was recorded using standard microelectrode technique prior to and after ablation. Before ablation, the action potentials recorded in the area of proposed lesion were exclusively from atrial or AN cells. At postablation, the superior margin of the lesion was populated with atrial or AN cells. AN, N, or NH cells bordered the lower part of the lesion. Electrophysiology of surviving cells at the edges of the lesion showed no significant changes in their V_{max}, APD_{50} or APD_{90} and MDP from preablation values. Fast AV node pathway input ablation in the rabbit heart can be accomplished with a singular lesion around the atrial insertion site of the tendon of Todaro, involving atrial or AN cells. The results of the studies imply that inputs to the compact node may act as a substrate for successful ablation of AV node reentry tachycardia.

Key Words: *Tachycardia, Atrioventricular Nodal Reentry; Catheter Ablation, Radiofrequency; Electrophysiology*

Kyung Hee Yi, Heon-Seok Han

Department of Pediatrics, Chungbuk National University, College of Medicine, Cheongju, Korea

Received: 3 January 2000
Accepted: 15 June 2000

Address for correspondence
Heon-Seok Han
Department of Pediatrics, Chungbuk National University, College of Medicine, San 48, Gaesin-dong, Heungdeok-gu, Cheongju 361-711, Korea
Tel: +82.43-269-6370
E-mail: hshan@med.chungbuk.ac.kr

INTRODUCTION

While atrioventricular nodal reentry tachycardia (AVNRT) is a common etiology in adult supraventricular tachycardia (SVT), it is responsible for only 10 to 15% in childhood SVT (1, 2). The advent of radiofrequency ablation technique has led to an increased interest in correlation of structure and function with respect to atrioventricular node (AVN) conduction. Treating tachycardia with radiofrequency ablation showed that antegrade AV node conduction is composed of fast and slow components with specific anatomic locations within the triangle of Koch. AVNRT would improve if either pathway, the circuit of tachycardia, was destroyed. Radiofrequency energy delivered near the mouth of the coronary sinus in triangle of Koch (posterior atrial input of the AVN) has been shown to destroy slow antegrade AV nodal conduction, thus eliminating the substrate responsible for AVNRT (3, 4). However, detailed cellular electrophysiologic data concerning ablation effects in specific areas of the triangle of Koch using AV node tissue are not available. Interest in antegrade slow conduction has also raised additional questions about other possible anatomic regions of input to AVN. Combined morphologic and electrophysiological studies of the rabbit AVN by Anderson et al. have shown that there are three separate atrial input areas to AVN (anterior, middle, and posterior) which can be anatomically defined (5). Furthermore, they correlated these input areas with specific histologic findings and cellular electrophysiologic parameters.

The purpose of this study is to investigate, using ablation technique, the cellular electrophysiology of the region of ablation prior to and after the elimination of fast pathway input (anterior approach) of antegrade AVN conduction. We hypothesize that this specific atrial input area makes a distinct predictable contribution to antegrade AVN conduction. Furthermore, modifying atrial input will result in definable electrophysiologic effects with corresponding histologic and morphologic changes to the AVN region. The contribution of this anatomic input towards the physiology of antegrade conduction will be quantified by using radiofrequency energy to modify atrial inputs. Similarly, the exact insertion of this input as they relate to the architecture of the post-ablation AVN will be clarified. It is important to define the relationships of the lesioned atrial input to the transitional open zone of the AVN, as well as the compact node. This information may help solve the controversy

as to whether slow and fast components of the circuit of AVNRT exclusively involve transitional and compact regions of the AVN, perinodal atrial tissues, or both.

MATERIALS AND METHODS

The experiment was conducted as follows: 1) AVN tissue preparation 2) Definition of preablation extracellular and intracellular AVN electrophysiology 3) Ablation of fast pathway atrial input 4) Redefinition of postablation AVN extracellular and intracellular electrophysiology.

Tissue preparation

Adult New Zealand white rabbits, weighing 2.0-2.5 kg, were anesthetized with 60 mg/kg pentobarbital sodium injected intravenously into a marginal ear vein along with 1,000 U/kg of heparin sulfate. The chest was opened with mid-sternal incision and the heart was removed and placed in cold modified Krebs buffer solution for dissection. The ventricle below the AV ring was removed and the right atrium was opened by making an incision through the AV ring and along the margin of the atrial appendage. A razor blade was used to trim excess atrial and ventricular myocardium away from the mouth of the coronary sinus and AVN structures. The preparation was then placed, endocardial side up, in a small Lucite superfusion bath. Modified Krebs solution was composed of mmol/L: NaCl, 141; KCl, 2.6; $MgSO_4$, 1.2; KH_2PO_4, 1.2; HEPES, 10; dextrose, 11. The solution was saturated with 100% O_2 and warmed to 37℃, superfusing the tissue at a flow rate of 12 mL/min.

Extracellular electrophysiologic evaluation

Bipolar stimulus and recording electrodes were constructed respectively from 30 g (nominally 0.33 mm in diameter) and 34 g (nominally 0.18 mm in diameter) of teflon-coated silver wire (Cooner Wire, Chatsworth, CA, U.S.A.) tightly twisted together. A stimulus electrode was placed on the atrial septum posterior to the foramen ovalis. The atrial electrogram (AEG) electrode was placed on the atrial septum immediately above the coronary sinus. The His electrogram (HEG) was recorded from the A-V groove anterior to the coronary sinus. Stimulation pulses were produced by D/A pulses from a microcomputer-based I/O board and Lab Windows software (AT-MIO-64F-5, National Instruments, Austin, TX, U.S.A.). In all the experiments, the basic cycle interval (S1-S1) was 600 msec and the stimulus duration was 1 msec. The stimulus amplitude was adjusted to 2X threshold. AVN recovery curve was obtained by premature pacing protocol. After 8 S1 pulses, a premature stimulus (S2) was delivered. The premature interval was initially decremented by 20 msec at the longest coupling intervals. As the premature coupling intervals became shorter the decrements were successively reduced to a minimum of 5 msec. Plots were made from recovery interval on X axis and conduction time on Y axis. For AVN conduction, the A2-H2 interval was plotted versus the nodal recovery (H1-A2). In this graph, minimum conduction time (AH_{min}) was defined as the shortest conduction time during steady state pacing, and maximal conduction time (AH_{max}) was the longest premature conduction time. In most experiments, all conduction times were measured from the His electrogram.

Intracellular electrophysiologic evaluation

Cellular electrophysiology of each region was obtained using standard microelectrode techniques. Glass capillary microelectrodes, having a tip resistance of 15-25 MΩ, were filled with 3M KCl. The microelectrodes were inserted into different regions of the AVN. The microelectrodes were attached to the headstage of a negative capacitance electrometer (World Precision Instrument, KS-700) through an Ag-AgCl half-cell. An Ag-AgCl half-cell reference electrode was placed in the flow side of the bath. To identify and record the locations of lesions, a grid diagram was constructed. The amplified transmembrane signal was monitored on an oscilloscope and EVR-16 (Electronics for medicine, Overland Park, KS, U.S.A.). Data were digitized at 1 kHz and stored on a microcomputer hard disk for later analysis. The action potential records were analyzed using a computer program that determined the activation voltage, peak overshoot and maximum diastolic potential (MDP). The program then calculated the total amplitude (Amp) of each action potential, maximum rate of rise of phase 0 (V_{max}), and action potential duration at 50% repolarization (APD_{50}), and at 90% repolarization (APD_{90}). V_{max} was calculated using a first difference approximation of the first time differential (6). All other action potential measurements were marked on the computer screen and visually verified.

Radiofrequency lesioning technique

After collecting the AVN recovery curve, cellular electrophysiology of each region was recorded. Preablation cellular electrophysiology of each region was described as atrial (A), transitional (AN), nodal (N) and low nodal (NH) according to the location of the action potential upstroke with respect of the AEG and HEG deflection.

Because there was a rough continuum of action potential characteristics from the atrial myocardium to the His bundle, absolute action potential classification was difficult. The AN action potential upstroke occurred in the first 12 msec of AH interval during normal antegrade conduction. The N action potential upstroke occurred between 13 and 37 msec of the AH interval. The NH action potential upstroke occurred 38 msec or more after the AEG deflection (7). A bipolar ablation electrode was constructed from 36 g teflon coated platinum wire (World Precision Instrument, Sarasota, FL, U.S.A.). The teflon was removed back approximately 300 μm from the tip of this wire, and the bared wire was looped back on itself with fine forceps. This tip was further smoothed by using very fine emery cloth, producing a pair of smooth low resistance electrodes that can be attached to a micromanipulator and moved across the atrial surface without injuring the tissue. The interelectrode separation was approximately 200 μm. The electrogram from this electrode was monitored and recorded in the bipolar mode prior to ablation. A double-throw, double-pole switch converted the electrode from recording to lesioning mode by connecting one of the bipolar electrodes to the output of a Radionics (Burlington, MA, U.S.A.) radiofrequency generator (RFG-3A). Radiofrequency lesioning was performed in the unipolar mode using a silver wire electrode placed away from the tissue in the bath and connected to the ground of the radiofrequency generator. Electrode resistance with this configuration is typically 180-200 Ω. A radiofrequency pulse of 1 watt for 2 sec was used to produce lesions. For fast pathway input ablation, lesioning was made at the atrial insertion site of the tendon of Todaro. The expected electrophysiologic end-point of this lesioning pattern is an increase in A-H interval for approximately 50%.

After the end-point was achieved, a repeat extracellular electrophysiologic evaluation was performed. The repeated intracellular electrophysiologic evaluation on the viable tissue margins of the lesion was recorded.

Statistical analysis

Mean between groups was compared using ANOVA for repeated measures with a Bonferroni adjustment and when appropriate, Student's t-test for paired observation was utilized (8). A p-value of less than 0.05 was considered significant.

RESULTS

Effects of fast pathway ablation on antegrade AV nodal recovery curves

After fast pathway input ablation of six superfused rabbit AVN preparations, AH_{min} increased significantly by 76.62% from 51.33±11.5 msec to 90.66±18.47 msec. But other parameters of AVN function did not reveal significant changes (Table 1). The recovery curves prior to and after fast pathway input ablation showed three patterns as follows: Four preparations showed slow conduction enhanced (Fig. 1A), 1 showed slow conduction unchanged (Fig. 1B), and the other showed slow conduction truncated (Fig. 1C).

Effects of fast pathway ablation on Intracellular electrophysiology of AV nodal region

Prior to ablation, the action potentials recorded in the area of the proposed lesion around the tendon of Todaro were exclusively from atrial or AN (transitional) cells (Fig. 2). After ablation, the superior margin of the lesion was populated with cells whose electrophysiology categorized them as atrial or AN cell. The lower part of the lesion was bordered by cells, which were characterized as AN, N (nodal), NH (nodal-Hisian) (Fig. 3). The electrophysiology of the surviving cells at the edge of the lesion showed no significant changes in their V_{max}, APD_{50}, APD_{90}, or MDP from preablation values (Table 2).

Table 1. Changes in extracellular electrophysiology of AVN prior to and after fast pathway ablation

Case	AH_{min}*		AH_{max}		⊿ AH		AVN ERP	
	Preablation	Postablation	Preablation	Postablation	Preablation	Postablation	Preablation	Postablation
1	41	62	114	179	73	117	125	164
2	55	89	113	146	58	57	110	105
3	64	91	147	133	83	42	131	151
4	65	117	101	162	36	45	172	179
5	41	83	122	105	81	22	107	207
6	42	102	117	185	75	83	129	225
Total	51.33±11.50	90.67±18.47	119±15.37	151.67±30.08	67.67±17.84	61±33.98	129±23.30	171.83±42.61

⊿ AH, difference between AH_{min} and AH_{max}; ERP, effective refractory period
*p<0.005 between pre and postablation

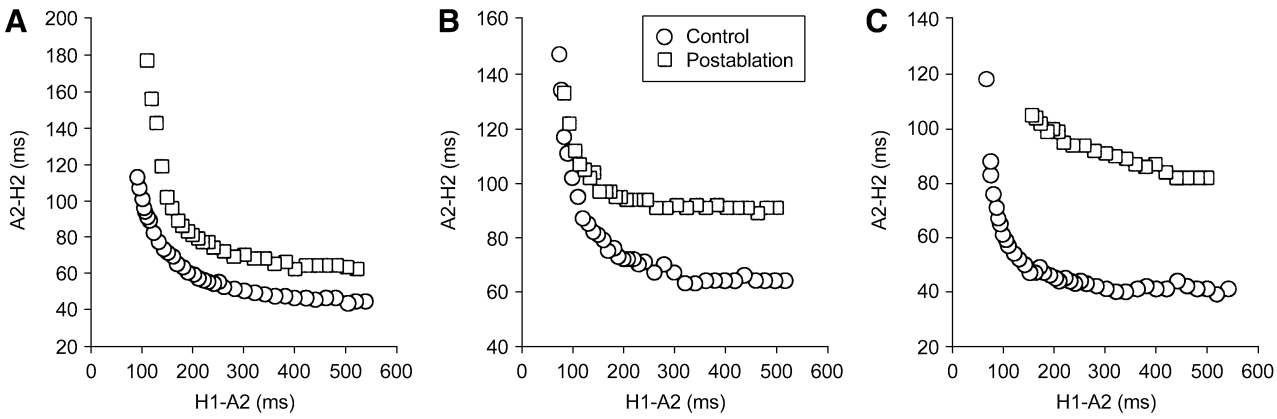

Fig. 1. AVN antegrade recovery curves prior to (circle) and after (rectangle) radiofrequency ablation of middle input to AVN. The basic cycle length in this experiment was 600 msec. Three figures show increased AH_{min} meaning modified fast conduction. A shows slow conduction enhanced, B shows slow conduction unchanged, and C shows slow conduction truncated.

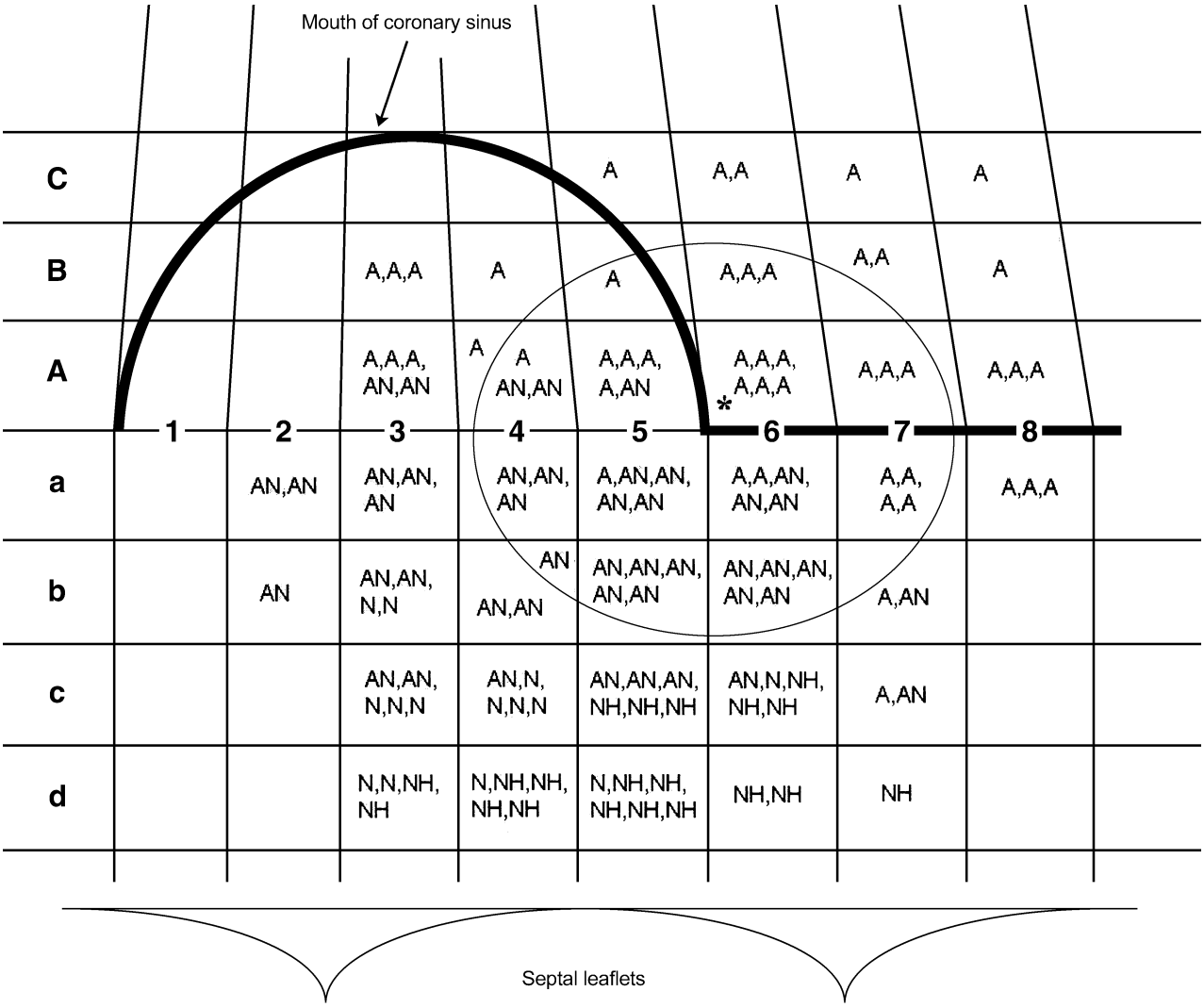

Fig. 2. A grid diagram of the mouth of coronary sinus used for locating intracellular electrophysiologic characteristics. The asterisk indicates the site at which radiofrequency ablation has resulted in the loss of fast conduction. The round area indicates proposed area of lesion. Followings are action potential characteristics; A, atria; AN, atrionodal; N, nodal; NH, nodal-Hisian. Note that the action potentials recorded in proposed ablation lesion include A or AN cells.

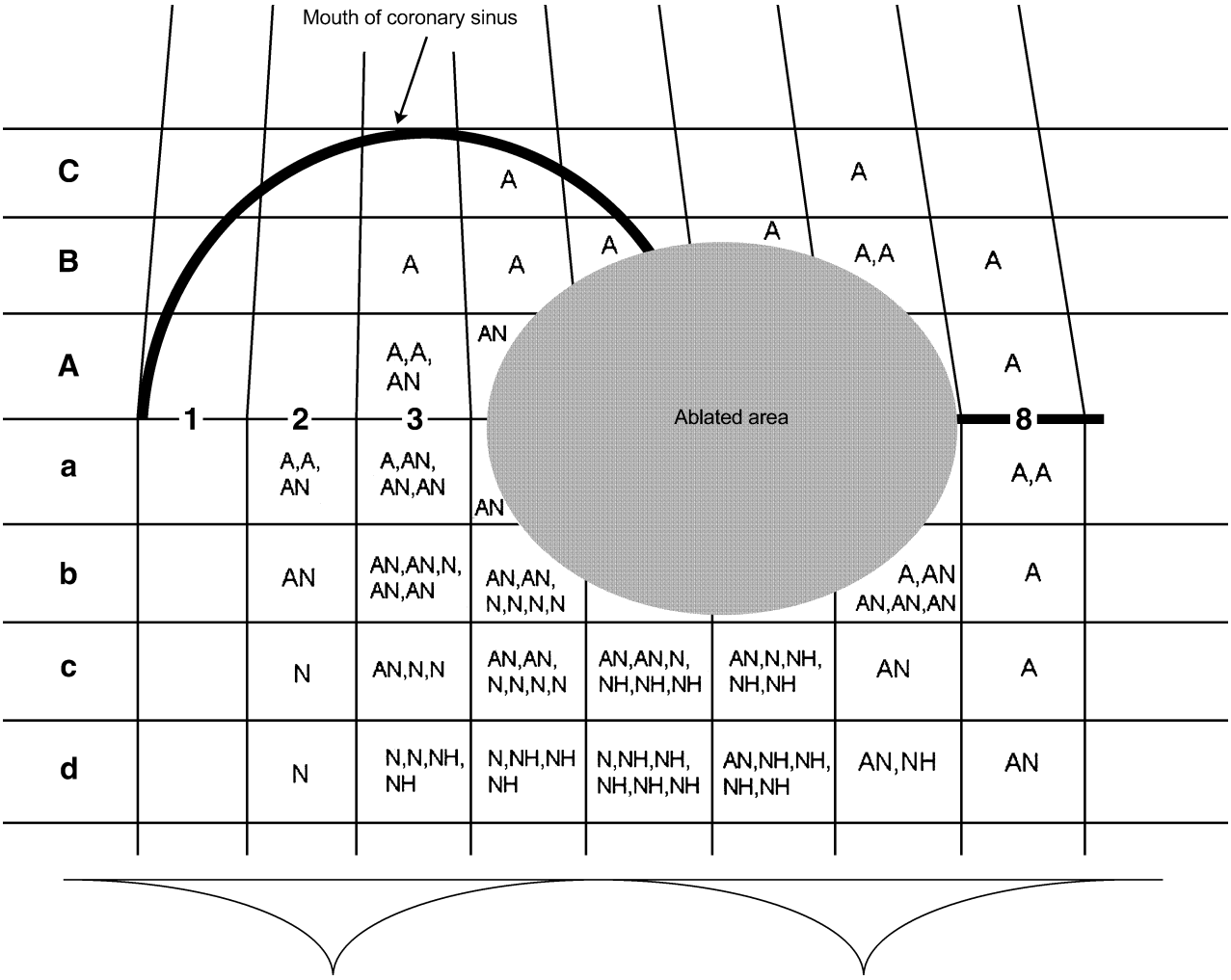

Fig. 3. A grid diagram of the mouth of coronary sinus used for locating intracellular electrophysiologic characteristics after radiofrequency ablation. The gray colored area is an ablated lesion. Note that the surviving cells around the lesion include A, AN, N, and NH cell.

Table 2. Changes in action potentials prior to and after fast pathway ablation

		Amp	V_{max}	APD_{50}	APD_{90}	MDP
AN cell	Preablation (intralesion) (n=24)	73±18	41±22	52±7	113±36	55±14
	Preablation (perilesion) (n=21)	75±11	46±27	47±5	100±30	58±10
	Postablation (perilesion) (n=28)	71±13	39±19	44±8	100±26	58±13
N cell	Preablation (n=14)	54±18	12±4	52±7	87±14	40±14
	Postablation (n=19)	61±8	13±8	51±5	91±13	50±16
NH cell	Preablation (n=20)	70±18	20±10	75±6	117±26	49±12
	Postablation (n-=21)	69±21	19±7	76±9	113±20	49±16

Intralesion: AN cell areas which will be ablated
Perilesion: AN cell areas which will be around the ablated lesion

DISCUSSION

Tawara first described anatomic and histologic structure of AVN, then Koch postulated that AVN was located within the triangle of Koch, which was constructed with membranous septum and septal leaflet of tricuspid valve, with the compact node located at the membranous septum (9). Further studies of electrical activity of AVN using microelectrode technique demonstrated that AVN consisted of three kinds of cells (10-12). They were characterized as AN, N, and NH according to their electrophysiologic activity. AN cells located

between atrium and compact node had varying resting potentials and upstroke action potentials from fast upstroke like atrial fiber to slow upstroke like N cells or sinus nodal cells. NH cells located between compact node and His bundle had high negative resting potentials and fast upstroke action potentials.

Mendez and his colleagues hypothesized the existence of dual atrioventricular nodal pathways to explain atrioventricular nodal echo complexes elicited in a rabbit model (13). They postulated existence of an antegrade slow conducting pathway with a shorter refractory period compared with a fast conducting pathway. Thus, premature impulses that were blocked in the fast pathway could conduct over the slow pathway and subsequently reenter the fast pathway to produce return impulses to the atrium. In this model, selective ablation of either pathway could prevent echo complexes or tachycardia. The advent of radiofrequency catheter ablation led to an increased interest in correlation of structure and function with respect to AVN conduction. Catheter ablation techniques have illustrated that antegrade AVN conduction is composed of fast and slow components with specific anatomic locations within the triangle of Koch (3, 4). Clinically, Lee et al. showed that radiofrequency lesion placed in the atrium just caudal to the area where the His bundle electrogram was recorded reproducibly resulted in selective ablation or modification of fast pathway function (14). Jackman et al. subsequently showed that ablative lesions placed between the coronary sinus os and the septal leaflet of the tricuspid valve selectively destroyed slow pathway function (15). However, detailed cellular electrophysiologic data concerning ablation effects in specific areas of the triangle of Koch using AV node tissue are not available.

In the previous experiment using four perfused rabbit hearts, fast conduction was increased across the AV node at long prematurity intervals an average of 67% in all preparations, while slow conduction was either preserved or enhanced in 3 of 4 preparations and lost in fourth preparation, after ablation of middle atrial input of the AV node (16). Chorro et al. studied electrophysiological effects of selective radiofrequency ablation in the anterior and posterior zone of the Koch's triangle using perfused rabbit heart. In the anterior zone the AH interval was prolonged to a greater extent, while in the posterior zone the effects were greater on the Wenckebach cycle length (17). We used superfused AV nodal tissue instead of perfused rabbit model to evaluate intracellular electrophysiology around the insertion site of tendon of Todaro. Similar to the previous perfused model, ablation of the middle input of AV node produced consistent changes in fast AV node conduction, and varied effects on slow conduction, ranging from elimination to enhancement of this AV node property. Among the antegrade AVN recovery curves after fast pathway input ablation, Fig. 1B would be theoretically ideal. However, varying effects on slow conduction are difficult to explain. According to Mendez et al., α and β pathways are only 0.3 to 0.5 mm apart (13). In view of the size of ablation lesion in our experiment, the ablation would have influenced both atrial input areas and the slow conduction would be enhanced or truncated by different degrees of atrial summation.

Josephson et al. suggested that the tachycardia circuit caused by atrioventricular nodal reentry mechanism was entirely intranodal (18). Data from humans suggest the atria are not necessary, including the presence of AV dissociation during supraventricular tachycardia, depolarization of atrial tissue surrounding the node without affecting SVT, pacing induced AH intervals exceeding those during SVT, and site dependency of a critical AH interval (exceeding atrial refractoriness) which is required for initiation of AV nodal tachycardia. However, others raised the possibility that atrial perinodal fibers are critical links in the tachycardia circuit (19). Iinuma et al. demonstrated that surgical interruption of the perinodal tissue prevented reinitiation of reentrant phenomena in superfused rabbit heart (20). Holman et al. also confirmed that atrioventricular node reentry tachycardia can be cured by dissecting atrial perinodal fibers without disrupting atrioventricular nodal conduction in animal experiment (21). Our results show that the ablated lesion include exclusively atrial or atrionodal cells and action potentials did not change significantly prior to and after ablation, suggesting that atrial perinodal fibers are critical links in the tachycardia circuit. Because our tissue did not show AV nodal echo or AVNRT before ablation, above suggestion may not be possible. But, increased fast pathway conduction after ablation suggests that at least fast pathway was modified by RF energy given at the atrial insertion site of tendon of Todaro. Our study had some limitations such as a small number of cases, and use of superfused isolated rabbit AV nodal tissue without effects of autonomic nervous influences. Therefore, our data are not applicable directly to the human heart.

In conclusion, discrete fast AV node pathway ablation in the rabbit can be accomplished with a singular lesion around the atrial insertion site of the tendon of Todaro. The cellular electrophysiologic characteristics of these areas involve atrial or atrionodal cells. The study implies that inputs to the compact node may act as the substrate for successful ablation of AV node reentry tachycardia.

REFERENCES

1. Garson A Jr, Gillette PC, McNamara DG. *Supraventricular*

tachycardia in children: clinical features, response to treatment, and long term follow-up in 217 patients. J Pediatr 1981; 98: 875-82.

2. Ko JK, Deal BJ, Strasburger JF, Benson DW Jr. *Supraventricular tachycardia mechanisms and their age distribution in pediatric patients. Am J Cardiol 1992; 69: 1028-32.*
3. Roman CA, Wang X, Friday KJ, Moulton KP, Margons PD, Klonis D, Calame J, Lazzara R, Jackman WM. *Catheter technique for selective ablation of slow pathway in AV nodal reentrant tachycardia [abstract]. Pacing Clin Electrophysiol 1990; 13: 498.*
4. Scheimman MM. *Atrioventricular reentry: lesson learned from radiofrequency modification of the node. Circulation 1992; 85: 1619-20.*
5. Anderson RH, Janse MJ, van Capelle FJ, Billette J, Becker AE, Durrer D. *A combined morphological and electrophysiological study of the atrioventricular node of the rabbit heart. Circ Res 1974; 35: 909-22.*
6. Buckles DS, Hewett KW. *Assessment of the maximum frequency components and digital sampling of cardiac Purkinje fiber action potentials. Comput Biomed Res 1986; 19: 410-6.*
7. Hewett KW, Gaymes CH, Noh CI, Ross BA, Thompson RP, Buckles DS, Gillette PC. *A cellular electrophysiology of neonate and adult rabbit atrioventricular node. Am J Physiol 1991; 260: H1674-84.*
8. Ludbrook J. *Repeated measurements and multiple comparisons in cardioventricular research. Cardiovasc Res 1994; 28: 303-11.*
9. Koch WL. *Weitere Mitteilunger Ueber den sinusknoten des herzens. Verh Dtsch Ges Pathol 1909; 13: 85-92.*
10. Meijler FL, Janse MJ. *Morphology and electrophysiology of the mammalian atrioventricular node. Physiol Rev 1988; 68: 608-47.*
11. Kokubun S, Neshimura M, Noma A, Irisawa H. *Membrane currents in the rabbit atrioventricular node cell. Pflugers Arch 1982; 393: 15-22.*
12. Noma A, Nakayama T, Kurachi Y, Irisawa H. *Resting K conductance in pacemaker and non-pacemaker heart cells of the rabbit. Jpn J Physiol 1984; 34: 245-54.*
13. Mendez C, Moe GK. *Demonstration of a dual A-V nodal conduction system in the isolated rabbit heart. Circ Res 1966; 19: 378-93.*
14. Lee MA, Morady F, Kadish A, Schamp DJ, Chin MC, Scheinman MM, Griffin JC, Lesh MD, Pederson D, Goldberg J, Calkins H, deBuitleir M, Kou WH, Rosenheek S, Sousa J, Langberg JJ. *Catheter modification of the atrioventricular junction with radiofrequency energy for control of atrioventricular nodal reentry tachycardia. Circulation 1991; 83: 827-35.*
15. Jackman WM, Beckman KJ, McClelland JH, Wang X, Friday KJ, Roman CA, Moulton KP, Twidale N, Hazlitt HA, Prior MI, Oren J, Overholt ED, Lazzara R. *Treatment of supraventricular tachycardia due to atrioventricular nodal reentry, by radiofrequency catheter ablation of slow-pathway conduction. N Engl J Med 1992; 327: 313-8.*
16. Case CL, Kahn IH, Le F, Thompson RP, Gillette PC, Hewett KW. *Electrophysiologic consequences of discrete lesioning of the putative middle atrial input of the rabbit atrioventricular node [abstract]. Pediatr Res 1994; 35: 31.*
17. Chorro FJ, Sanchis J, Such L, Artal L, Llavador JJ, Llavador E, Monmeneu JV, L'opez-Merino V. *Modification of atrioventricular nodal electrophysiology by selective radiofrequency delivery on the anterior or posterior approaches. Pacing Clin Electrophysiol 1997; 20(5 Pt 1): 1261-73.*
18. Josephson ME, Miller JM. *Atrioventricular nodal reentry: evidence supporting an intranodal location. Pacing Clin Electrophysiol 1993; 16(Pt II): 599-614.*
19. Janse MJ, Anderson RH, McGuire MA, Ho SY. *"AV nodal" reentry: Part 1: "AV nodal" reentry revisited. J Cardiovasc Electrophysiol 1993; 4: 561-72.*
20. Iinuma H, Dreifus LS, Mazgalev T, Price R, Michelson EL. *Role of the perinodal region in atrioventricular nodal reentry: evidence in an isolated rabbit heart preparation. J Am Coll Cardiol 1983; 2: 465-73.*
21. Holman WL, Ikeshita M, Lease JG, Ferguson TB, Lofland GK, Cox JL. *Alteration of antegrade atrioventricular conduction by cryoablation of periatrioventricular nodal tissue. Implications for the surgical treatment of atrioventricular nodal reentry tachycardia. J Thorac Cardiovasc Surg 1984; 88: 67-75.*